This full text paper was peer reviewed at the direction of IEEE Communications Society subject matter experts for publication in the IEEE ICC 2009 proceedings

Sub-noise primary user detection by cross-correlation

M. Heskamp, C. H. Slump
University of Twente, Faculty of EEMCS,
Signals and Systems Group (SaS),
P.O. box 217 - 7500 AE Enschede - The Netherlands
Phone: +31 53 489 2673 Fax: +31 53 489 1060
E-mail: m.heskamp@utwente.nl

***Abstract*—An ideal cognitive radio must be able to detect primary user signals under unfavorable conditions. Especially when the hidden node problem occurs, a cognitive radio is required to detect the presence of signals under the noise floor. This paper addresses the question to what extent sub-noise detection is practically usable in a cognitive radio. Three methods based on cross-correlation are analyzed and compared.**

I. Introduction

As Moore's law still holds, the digital signal processing capability of wireless devices steadily grows. On the other hand, the amount of free radio spectrum for these devices is only becoming scarcer. Therefore, future radios will likely have far more processing capability than needed for modulation and demodulation. The idea of *cognitive radio*, first proposed by Mitola [1] and later adopted by the FCC [2], is to use this over capacity of future radio receivers to make spectrum access more dynamical and efficient. An ideal cognitive radio must be able to detect primary user signals under unfavorable conditions within a short time. It is obvious that the performance of any detector assigned to this task is bounded by both fundamental and practical limitations. The most important limitation is noise. Noise in a radio receiver mainly consists of man-made and natural background noise, and noise added by the receiver itself. Once a signal is buried in noise, it becomes in principle undetectable, unless the noise can somehow be averaged out. The principle of noise reduction by averaging can appear in many forms. The main idea that is analyzed in this paper is that of having two copies of the signal, each corrupted by independent noise. In a cross-correlation between both copies, the noise term disappears, whereas the signal component converges to the power of the signal. A schematic of the cross-correlator is shown in Fig. 1.

We consider two methods of obtaining the two signal copies. One is based on cyclostationarity, where there are multiple copies of (part of) the signal on different frequencies, and the other uses two analog front-ends. The purpose of this paper is to explore the feasibility of detectors based on such second order statistics of a signal. The remainder of this paper is structured as follows. First we provide a short introduction to cyclostationarity, and explain how cyclostationarity may be present in a practical signal. Next, we analyze two schemes of detecting cyclostationarity, and compare them with cross-correlation between two front-ends.

[1]This work is supported by the Dutch Ministry of Economic affairs BSIK funding project and is part of the FreeBand program.

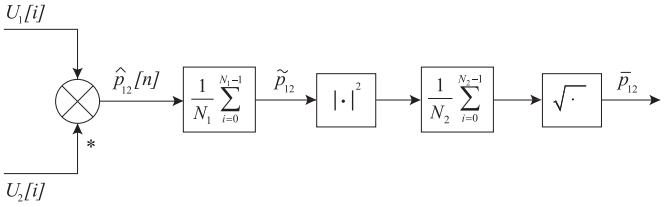

Fig. 1. Proposed cross-correlator scheme. The first averaging reduces the noise. Next the estimation is squared to make it positive, and a second averaging is applied to reduce the variance.

II. A review of cyclostationarity

In this paper we assume radio signals and noise to be realizations of zero mean Gaussian processes. Such a process is completely characterized by its autocorrelation function. The time dependent autocorrelation function of a signal $u(t)$ is defined as

$$R_{uu}(t,\tau) \;=\; \mathrm{E}\left\{u(t+\tfrac{1}{2}\tau)u^*(t-\tfrac{1}{2}\tau)\right\}. \qquad (1)$$

If $R_{uu}(t,\tau)$ is independent of t, the signal $u(t)$ is called stationary. It is called cyclostationary if there exist a $T>0$ such that

$$R_{uu}(t+T,\tau) \;=\; R_{uu}(t,\tau) \quad \forall t. \qquad (2)$$

The smallest $T>0$ for which (2) holds is called the cyclic period time T_{cycle}. If (2) holds only for $T=0$ the signal is called non-stationary. The sum of two or more cyclostationary signals is called poly-cyclostationary if the cyclic period times are not rational multiples of each other. If the signal is stationary, cyclostationary or poly-cyclostationary, the two dimensional Fourier transform

978-1-4244-3435-0/09/$25.00 ©2009 IEEE

$$R_{uu}(t,\tau) \qquad (t,\tau) \overset{\mathscr{F}^2}{\rightleftharpoons} (\alpha, f) \qquad S_{uu}(\alpha, f) \tag{3}$$

exists, in which $S_{uu}(\alpha, f)$ is called the *spectral correlation function* (SCF) [3]. The SCF is a generalized function, because it consists of delta functions, that appear as line masses parallel to the f axis. We can write the SCF therefore as

$$S_{uu}(\alpha, f) = \sum_{k=-\infty}^{\infty} S_{uu}^{k}(f)\delta(\alpha - \alpha_k). \tag{4}$$

If the signal is stationary, there is only one line mass on $\alpha = 0$, so that the SCF degenerates to the power spectral density (PSD)

$$R_{uu}(\tau) \qquad (\tau) \overset{\mathscr{F}}{\rightleftharpoons} (f) \qquad S_{uu}(f). \tag{5}$$

Since it is inconvenient to work with half sampling intervals, we use the following asymmetrical definition [1] [3]

$$\begin{aligned} R_{uu}[n,m] &= \mathrm{E}\left\{u[n]u^*[n-m]\right\} \\ [n,m] &\overset{\mathscr{F}^2}{\rightleftharpoons} (\alpha, f) \qquad S_{uu}(\alpha, f + \tfrac{1}{2}\alpha). \end{aligned} \tag{6}$$

If we omit the expectation operator in (6) we have

$$\hat{R}_{uu}[n,m] = u[n]u^*[n-m] = R_{uu}[n,m] + \Lambda[n,m] \tag{7}$$

in which $\Lambda[n,m]$ is a zero mean random process that represents the noise of the estimator. Since this noise is neither periodical or transient, its Fourier transform does not converge, and therefore also the Fourier transform of $\hat{R}_{uu}[n,m]$ does not exist. A practical implementation for measuring $S(\alpha, f)$ therefore has to perform two main tasks. First, it must limit the extend of the signal, which will lead to a convolutional smoothing effect in the frequency domain. Secondly, the noise must be reduced by averaging.

III. Cyclostationarity in practical signals

A typical signal type that can be encountered in the UHF band is TETRA [4]. TETRA is a modern digital trunked radio standard, mainly used in Europe in the 400 and 800 MHz band. If a cognitive radio is to be allowed in these bands, it certainly has to be able to detect and avoid TETRA channels, because they are often used by critical services such as ambulance and police. TETRA uses a 25 kHz wide channel and $\pi/4$-QPSK modulation with a symbol rate of 18k symbols/s. At baseband the TETRA signal can be written as

$$u(t) = \sum_{n=-\infty}^{\infty} c[n] \cdot g(t - nT) \tag{8}$$

[1]The square brackets distinguishes it from the symmetrical definition.

in which $c[n]$ are the complex data symbols, $g(t)$ is the pulse shape, and T the symbol duration time. The autocorrelation function at baseband is given by

$$R_{uu}(t,\tau) = g(t + \tfrac{1}{2}\tau)g^*(t - \tfrac{1}{2}\tau) \;*\; \frac{1}{T}\,\mathrm{III}(t/T) \tag{9}$$

in which III() denotes the unit pulse train. The two dimensional Fourier transform gives the SCF

$$S_{uu}(\alpha, f) = G(f + \tfrac{1}{2}\alpha)G^*(f - \tfrac{1}{2}\alpha) \cdot \mathrm{III}(\alpha T) \tag{10}$$

which is graphically depicted in Fig. 2.

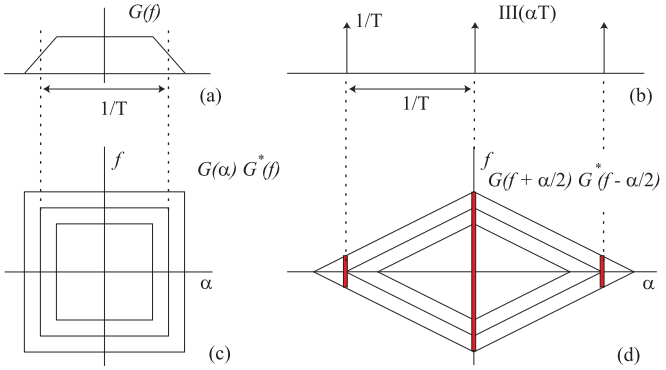

Fig. 2. Graphical representation of (10). (a) Frequency response of a Nyquist Pulse Shape, (b) Pulse train function, (c) Pulse Shape in the (α, f) plane, (d) The SCF of a PAM signal. The red lines are the cyclostationary features.

IV. Correlation between two DFT bins

In a cyclostationary signal there is correlation between two or more sub-bands of the signal. Therefore, we expect that there also will be correlation between DFT frequency bins. The idea of correlating between DFT bins was introduced in the cognitive radio field by Cabric et al. [5].

Let us review what happens if we correlate between two DFT bins, which we obtain with the schematic in Fig. 3. Please note that in the schematic, the mixer is a quadrature mixer, and double lines indicate analog quadrature pairs. In the digital domain, after the ADC, we consider all signals complex.

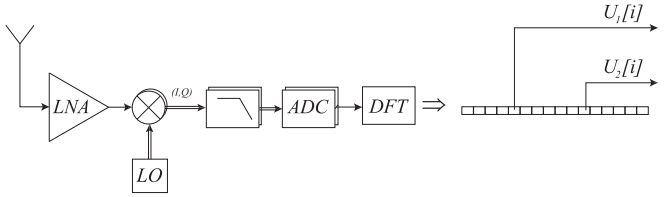

Fig. 3. Correlating between two DFT bins

We can write the output of the DFT as the following discrete time Fourier transform (DTFT)

$$U(i,f) = \sum_{n=0}^{L-1} w[n]u[n+i]\exp(-j2\pi fn) \tag{11}$$

in which $w[n]$ is a data window with length L, and i an arbitrary integer shift of the time origin. This Fourier transform can be interpreted as a DFT by only evaluating it on discrete values of its parameter, i.e. $f = \frac{k}{L}$ with $k = 0 \ldots L-1$.

The product between a DFT bin and the complex conjugate of another bin is

$$\begin{aligned} U(i,f_1)\cdot U^*(i,f_2) = \\ \sum_{n_1=-\infty}^{\infty}\sum_{n_2=-\infty}^{\infty} w[n_1]w^*[n_2]u[n_1+i]u^*[n_2+i] \quad \times \\ \exp(-j2\pi(f_1n_1 - f_2n_2)). \end{aligned} \tag{12}$$

Next, we change the variables to $n_1 = n$, $n_2 = n-m$ and $f_1 = f+\alpha$, $f_2 = f$. Note that since $\alpha = f_1 - f_2$ its range extends from -1 to 1, whereas f ranges from -0.5 to 0.5. With these new variables the product of the two bins becomes

$$\begin{aligned} U(i,f+\alpha)\cdot U^*(i,f) = \\ \sum_{n=-\infty}^{\infty}\sum_{m=-\infty}^{\infty} w[n]w^*[n-m]\hat{R}_{uu}[n+i,m] \quad \times \\ \exp(-j2\pi mf)\exp(-j2\pi n\alpha). \end{aligned} \tag{13}$$

This expression is the two dimensional Fourier transform

$$w[n]w^*[n-m]\hat{R}_{uu}[n+i,m] \quad \overset{\mathscr{F}^2}{\Longrightarrow} \quad U(i,f+\alpha)\cdot U^*(i,f) \tag{14}$$

which is related to the spectral correlation function by

$$\begin{aligned} U(i,f+\alpha)\cdot U^*(i,f) \quad = \\ W(f+\alpha)W^*(f) * \left(S_{uu}(\alpha, f+\tfrac{1}{2}\alpha)\exp(j2\pi\alpha i)\right) \\ + \quad \mathscr{F}^2\left[w[n]w^*[n-m]\Lambda[n+i,m]\right]. \end{aligned} \tag{15}$$

This estimation, formed by multiplying two DFT bins, has the following problems. First we see that a noise term Λ is present which has to be removed by averaging. Secondly, we have a phase rotation if we shift the time origin. If we want to average over time we have to compensate for this phase rotation, because otherwise the averaging will become incoherent. Thirdly, we see that the SCF is blurred because of the finite window length. This can be improved by increasing L . However, it is unfavorable to make L much larger than the function $R[n,m]$ extends in the m direction, because then we capture relatively much noise.

Let us see what happens if we average (15) without correcting the phase rotation. If we average over N_1 transforms that are shifted in time with step size P we get

$$\begin{aligned} \frac{1}{N_1}\sum_{i=0}^{N_1-1} U(iP,f+\alpha)\cdot U^*(iP,f) \quad = \\ W(f+\alpha)W^*(f) * (S(\alpha, f+\tfrac{1}{2}\alpha)\frac{1}{N_1}\sum_{i=0}^{N_1-1}\exp(j2\pi\alpha iP)) \\ + \quad \mathscr{F}^2\left[w[n]w^*[n-m]\frac{1}{N_1}\sum_{i=0}^{N_1-1}\Lambda[n+iP,m]\right]. \end{aligned} \tag{16}$$

Note that we can move the summation into the convolution and Fourier transform, because of linearity of these operations. The standard deviation of the noise term decreases with $N^{-0.5}$, which is 5 dB per factor 10 more averaging. However, for the averaging to work well, we require:

$$\begin{aligned} \frac{1}{N_1}\sum_{i=0}^{N_1-1}\exp(j2\pi\alpha iP) \quad = \\ \frac{1}{N_1}\frac{\sin(\pi\alpha PN)}{\pi\alpha P}\exp(j\pi\alpha P(N-1)) \quad = \quad 1 \end{aligned} \tag{17}$$

which only happens if α P is an integer. Therefore, this requirement can not be met for all values of α, so instead we require it to only hold on values where the cyclostationary features appear.

With a cyclic period time T_{cycle} and a sampling time t_s, the cyclic features occur on integer multiples of $\alpha = \frac{t_s}{T_{\text{cycle}}}$. From this, it follows that (17) holds if $t_s = k\frac{T_{\text{cycle}}}{P}$ in which k is an arbitrary integer. This means that we have to carefully match the sampling clock of our detector with the symbol clock of the target signal. This is an important disadvantage, because such an adjustable sampling clock means extra hardware costs. Furthermore, this adjustment of the sampling clock can only be done for one specific cyclostationary component, and not for multiple cyclostationary signals simultaneously.

Furthermore, since there is no obvious way to synchronize to a signal yet to be detected, we are likely to make an error in estimating the symbol timing. So, assume we make a relative error ϵ in estimating T_{cycle} so that our actual sampling time becomes

$$t_s' = \frac{T_{\text{cycle}}(1+\epsilon)}{P}. \tag{18}$$

Substituting this in (17) gives a residual attenuation of

$$\frac{1}{N_1}\sum_{i=0}^{N_1-1}\exp(j2\pi i\epsilon) \tag{19}$$

so that the averaging remains coherent as long as $N \ll |\epsilon|^{-1}$. If $N = |\epsilon|^{-1}$ the features are completely canceled, so we apply a factor of 10 back-off

$$N_{\max} \approx \frac{1}{10\epsilon}. \quad (20)$$

The performance for various accuracies is shown in table I.

ϵ	$N_{\max}$	dB	Acquisition Time
10 %	1	0	256 μs
1 %	10	5	2.56 ms
0.1 %	100	10	25.6 ms
100 ppm	1000	15	256 ms
10 ppm	1E4	20	2.56 s
1 ppm	1E5	25	25.6 s

TABLE I
NOISE REDUCTION FOR VARIOUS SAMPLING TIME ACCURACIES

The third column gives an indication of the noise suppression if we apply the 5 dB per factor 10 rule. The last column gives an indication of the acquisition time if we sample at 4 MHz and average over DFT blocks of 1024 samples.

If we make no effort to adjust the sampling clock, ϵ is a random variable that is uniformly distributed between -0.5 and 0.5. If we insert ϵ as a random variable in (19) and (20) and take the expectation, we see that they both become zero, so this method is unlikely to work without clock adjustment

V. CORRELATION BETWEEN TWO FREQUENCY BANDS

In the previous section we saw that correlating between DFT bins only works well if we adjust the sampling clock of the detector to the symbol clock of the target signal. Without this synchronization the SCF is averaged incoherently. This problem is caused by the fact that the resolution of the α parameter is limited by the width of the DFT bins. In the following scheme, which was introduced by Gardner [3], we can adjust α continuously.

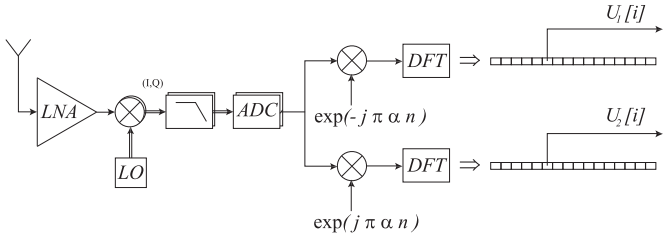

Fig. 4. Correlation between two frequency bands

The multiplication of the two DFTs is given by

$$U_1(i,f)U_2^*(i,f) = \sum_{n_1=-\infty}^{\infty}\sum_{n_2=-\infty}^{\infty} w[n_1]u[n_1+i] \quad \times$$
$$\exp(-j\pi\alpha(n_1+i))\exp(-j2\pi f n_1)$$
$$\times \quad w^*[n_2]u^*[n_2+i]\exp(-j\pi\alpha(n_2+i))\exp(j2\pi f n_2) \quad (21)$$

which is related to the SCF by

$$U_1(i,f)U_2^*(i,f) =$$
$$\exp(-j2\pi\alpha i)(W(f+\tfrac{1}{2}\alpha)W^*(f-\tfrac{1}{2}\alpha) * [S(\alpha,f)\exp(j2\pi\alpha i)])$$
$$+ \quad \mathscr{F}^2\left[w[n+\tfrac{1}{2}m]w^*[n-\tfrac{1}{2}m]\Lambda[n+\tfrac{1}{2}m+i,m]\right]. \quad (22)$$

Next, we insert (4) so that we can see what happens to the delta functions:

$$U_1(i,f)U_2^*(i,f) = \sum_{k=-\infty}^{\infty}\exp(-j2\pi(\alpha-\alpha_k)i)$$
$$W(f+\tfrac{1}{2}(\alpha-\alpha_k))W^*(f-\tfrac{1}{2}(\alpha-\alpha_k)) * S^k(f)$$
$$+ \quad \mathscr{F}^2\left[w[n+\tfrac{1}{2}m]w^*[n-\tfrac{1}{2}m]\Lambda[n+\tfrac{1}{2}m+i,m]\right]. \quad (23)$$

Now assume we make the window length L long enough, so that the width of the kernel $W(f)$ is much narrower than the distance between the delta function in the SCF. Then, if we tune α to some specific α_k, we get only one term of the summation in (23)

$$U_1(i,f)U_2^*(i,f)|_{\alpha=\alpha_k} \quad = \quad |W(f)|^2 * S^k(f)$$
$$+ \quad \mathscr{F}^2\left[w[n+\tfrac{1}{2}m]w^*[n-\tfrac{1}{2}m]\Lambda[n+\tfrac{1}{2}m+i,m]\right]. \quad (24)$$

It is clear that we can reduce the noise term by averaging with 5 dB per factor 10. Furthermore, it is clear that if we make a relative error ϵ in setting α to α_k we get the following attenuation after averaging:

$$\frac{1}{N_1}\sum_{i=0}^{N_1-1}\exp(j2\pi i\epsilon) \quad (25)$$

which is similar to the clock frequency error of the previous method. The advantage if this method is that α can be adjusted much more easily than the sampling clock. However, the performance of both methods is similar, and depends on knowing T_{cycle} accurately.

VI. CROSS-SPECTRUM BETWEEN TWO LNAS

The methods discussed in the two previous sections only worked if the detector was adjusted to the locations of the delta functions in the SCF, which is difficult in practice. However, one of the delta functions in the SCF is very easy to find, because if appears at $\alpha = 0$. This is in fact the power spectral density, which represents the stationary part of the signal. The problem with the PSD is that most of the noise is also stationary, so the PSD is often dominated by noise. A significant part of the noise is produced by the LNA of the receiver. Now, if we use two LNAs as shown in Fig. 5, we can

average out this noise. In order to keep both signals coherent, the mixers in both front-ends is driven by the same oscillator. Also note that we initially lose 3 dB SNR by splitting the antenna signal.

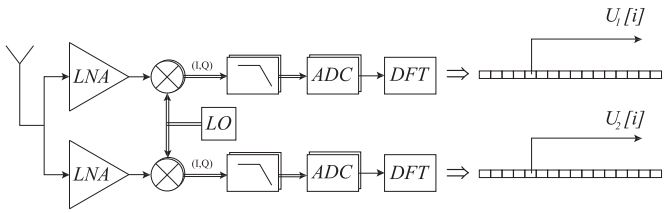

Fig. 5. Correlation between two front-ends

If we insert $\alpha = 0$ in (24) and apply averaging with step size P over N_1 DFTs, we get

$$\frac{1}{N_1}\sum_{i=0}^{N_1-1} U_1(iP,f)U_2^*(iP,f) \;=\; |W(f)|^2 \;*\; S(f)$$

$$+\,\mathscr{F}^2\left[w[n+\tfrac{1}{2}m]w^*[n-\tfrac{1}{2}m]\frac{1}{N_1}\sum_{i=0}^{N_1-1}\Lambda[n+\tfrac{1}{2}m+iP,m]\right] \tag{26}$$

which shows that we can reduce the noise by 5 dB per factor 10 averaging, without coherency problems.

Next, we have a closer look at how the variance is reduced by averaging. To simplify the analysis, we assume that the subsequent output samples of the DFT are uncorrelated. This happens if we make L sufficiently large, i.e. larger than the extend of $R[n,m]$ in the m direction. We also set the averaging step size conveniently to $P = L$. For the DFT output samples at a certain bin number k we use the following shorthand notation

$$U_1[i] = U_1(iL,k/L) \quad \text{and} \quad U_2[i] = U_2(iL,k/L). \tag{27}$$

The DFT bins of the two paths contain a common signal component $U[i]$, and different noise components $x_1[i]$ and $x_2[i]$

$$U_1[i] = U[i] + x_1[i] \quad \text{and} \quad U_2[i] = U[i] + x_2[i]. \tag{28}$$

The sequences $U[i]$, $x_1[i]$ and $x_2[i]$ are assumed to be independent, white, zero-mean Gaussian processes with variances p_u, p_{x_1} and p_{x_2} respectively. Each complex variable is assumed to have an independent real and imaginary part with equal variance. Because the noise is uncorrelated we can average it out if we cross-correlate between both channels. From one sample of each channel we form the product:

$$\hat{p}_{12} \;=\; U_1 \cdot U_2^* \;=\; |U|^2 + Ux_2^* + U^*x_1 + x_1x_2^*. \tag{29}$$

The expectation of this product is

$$\mathrm{E}\{\hat{p}_{12}\} \;=\; \mathrm{E}\{U_1 \cdot U_2^*\} \;=\; \mathrm{E}\{|U|^2\} = p_u. \tag{30}$$

In order to find the variance, we first determine the second order moment

$$\begin{aligned}\mathrm{E}\{|\hat{p}_{12}|^2\} \;=\; \mathrm{E}\{\quad & (|U|^2 + Ux_2^* + U^*x_1 + x_1x_2^*) \\ \times\quad & (|U|^2 + U^*x_2 + Ux_1^* + x_1^*x_2)\quad\}.\end{aligned} \tag{31}$$

For zero mean Gaussian variable the following well known rule applies:

$$\mathrm{E}\{abcd\} = \mathrm{E}\{ab\}\,\mathrm{E}\{cd\} + \mathrm{E}\{ac\}\,\mathrm{E}\{bd\} + \mathrm{E}\{ad\}\,\mathrm{E}\{bc\}. \tag{32}$$

If we apply this rule to (31) we see that most of the terms are zero, except those that contain two pairs of correlating variables

$$\mathrm{E}\{|\hat{p}_{12}|^2\} = 2p_u^2 + p_up_{x_1} + p_up_{x_2} + p_{x_1}p_{x_2} \tag{33}$$

so for the variance we have

$$\mathrm{VAR}\{\hat{p}_{12}\} \;=\; (p_u + p_{x_1})(p_u + p_{x_2}). \tag{34}$$

If the noise is zero, we see that the variance becomes equal to the square of the mean, which is consistent with the fact that for zero noise $\hat{p}_{12}$ becomes exponentially distributed.

A. Averaging

From (30) and (34) we see that the estimation $\hat{p}_{12}$ based on a single pair of samples it too noisy to be useful. In fact the standard deviation is larger than the expected value. To reduce the variance we apply averaging over N_1 samples:

$$\tilde{p}_{12} = \frac{1}{N_1}\sum_{i=0}^{N_1-1} U_1[i]U_2^*[i]. \tag{35}$$

This averaging does not change the expectation, but the variance is reduced to

$$\mathrm{VAR}\{\tilde{p}_{12}\} \;=\; \frac{1}{N_1}(p_u + p_{x_1})(p_u + p_{x_2}). \tag{36}$$

On a logarithmic power scale we see that the noise drops 5 dB if the averaging length is increased by a factor of 10. So, by increasing N_1 we can lower the noise below any limit, provided that we have enough time, and all involved signals remain stationary.

B. Smoothing the noise floor

The estimation $\tilde{p}_{12}$, obtained by cross-correlation, is not non-negative and can even be complex, which is undesirable for a power estimation. To correct this we take its squared magnitude. If N_1 is not too small, $\tilde{p}_{12}$ is approximately Gaussian distributed with a mean of p_u and variance given by and (36). The mean after squaring is easily found to be

$$\mathrm{E}\left\{|\tilde{p}_{12}|^2\right\} \quad = \quad p_u^2 \quad + \quad \frac{(p_u + p_{x_1})(p_u + p_{x_2})}{N_1} \qquad (37)$$

and the variance after squaring is

$$\mathrm{VAR}\{|\tilde{p}_{12}|^2\} \quad = \quad \left(\mathrm{E}\left\{|\tilde{p}_{12}|^2\right\}\right)^2 \quad - \quad p_u^4. \qquad (38)$$

From (37) we see that we now have a bias, but in return get positive power values. Finally, we apply a second averaging step over length N_2 to smooth out the remaining noise, so that the final estimation becomes

$$\bar{p}_{12} = \sqrt{\langle\ |\tilde{p}_{12}|^2\ \rangle_{N_2}}. \qquad (39)$$

We can summarize the output of the second averager by considering two cases. First, if the signal is relatively strong we have

$$\mathrm{E}\left\{\bar{p}_{12}^2 \quad | \ p_{x_1} \approx p_{x_2} \approx 0\right\} \quad \approx \quad p_u^2, \qquad (40)$$

$$\mathrm{STD}\{\bar{p}_{12}^2 \quad | \ p_{x_1} \approx p_{x_2} \approx 0\} \quad \approx \quad \frac{\sqrt{2}}{\sqrt{N_1 N_2}} p_u^2. \qquad (41)$$

Secondly, if the signal is very weak we have the following noise floor:

$$\mathrm{E}\left\{\bar{p}_{12}^2 \quad | \ p_u \approx 0\right\} \quad \approx \quad \frac{p_{x_1} p_{x_2}}{N_1}, \qquad (42)$$

$$\mathrm{STD}\{\bar{p}_{12}^2 \quad | \ p_u \approx 0\} \quad \approx \quad \frac{p_{x_1} p_{x_2}}{N_1 \sqrt{N_2}}. \qquad (43)$$

C. Setting the threshold level

Finally we can derive an expression for the detection threshold λ. We can set the threshold to the expected noise floor plus a margin of β times the standard deviation. This will give

$$\lambda^2 = \frac{p_{x_1} p_{x_2}}{N_1} + \beta \frac{p_{x_1} p_{x_2}}{N_1 \sqrt{N_2}}. \qquad (44)$$

On a decibel scale this gives

$$\mathrm{dB}_\lambda = p_x(\mathrm{dB}) - 5\log(N_1) + \frac{5\beta}{\ln(10)\sqrt{N_2}}. \qquad (45)$$

VII. Discussion and conclusions

In this paper a theoretical analysis is made of three methods of sub-noise detection based on cross-correlation. All such methods provide 5 dB noise reduction per factor ten increase of averaging length. Since for cognitive radio detection has to occur in a fraction of a second, it is expected that the maximum realizable noise reduction will in practice not be much more than about 15 dB. It was also observed that the noise floor in a cross-spectrum is very erratic. Because algorithms for establishing the detection threshold need a steady noise floor, a second averaging is needed to smooth out the noise floor. The total averaging time will roughly be equal to the product of both averaging times. The two methods based on cyclostationarity can work in theory if the detector is closely tuned to the cyclic frequency of the target signal. In practice, however, such tuning is difficult and likely not robust. Furthermore, in practice the target bandwidth may contain a whole ensemble of signals with different parameters, which all have to be sensed for. This makes the cyclostationary method even more unpractical. The two front-end approach, on the other hand, seems promising, and may provide a viable way to relieve the requirement of the analog part of the spectrum sensing receiver.

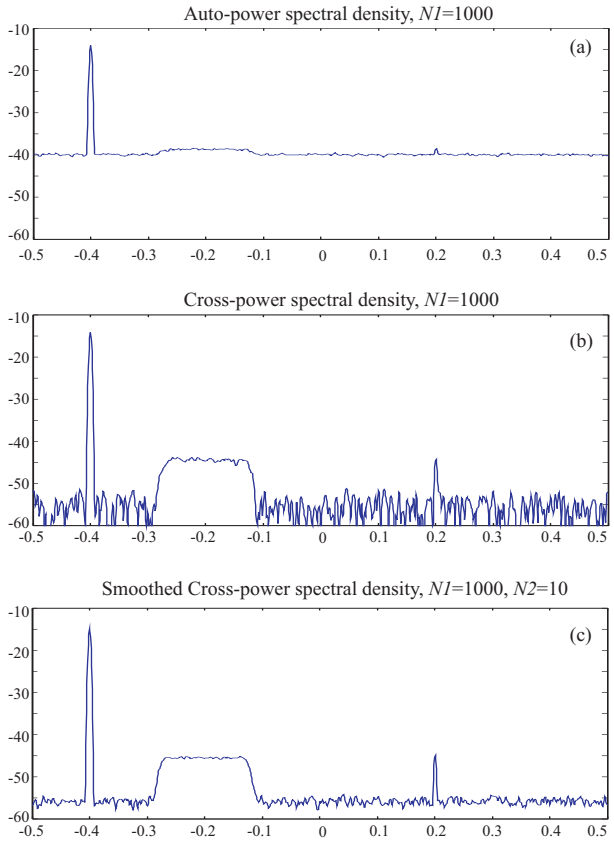

Fig. 6. Simulation results with a strong and a weak carrier waves, and a weak QAM signal. (a) shows the PSD if only one front-end is used. Only the strong carrier signal is visible. (b) shows that cross-spectrum between two front-ends. (c) shows how the noise floor is smoothed by the second averager.

References

[1] J. Mitola III, "Cognitive radio: An integrated agent architecture for software defined radio," Ph.D. dissertation, Royal Institute of Technology (KTH), Stockholm, 2000.

[2] FCC, "Facilitating opportunities for flexible, efficient, and reliable spectrum use employing cognitive radio technologies," ET Docket No. 03-108, December 2003, notice of Proposed Rulemaking (NPRM).

[3] W. A. Gardner, *Cyclostationarity in Communications and Signal Processing*. IEEE Press, 1994.

[4] ETSI, "Terrestrial trunked radio; voice plus data; part 2: Air interface," European Standard EN 300 392-2, 2006.

[5] D. Cabric, S. Mishra, and R. Brodersen, "Implementation issues in spectrum sensing for cognitive radios," *Thirty-Eighth Asilomar Conference on Signals, Systems and Computers*, vol. 1, pp. 772 – 776, Nov 2004.